

where \mathcal{E}_F is the fluctuation level ($= E_y^2/8\pi$ averaged in the sheath), Z is the plasma dispersion function, $\xi_i = \omega/kv_i$, v_i is the ion thermal velocity, and $\omega = \omega_R + i\gamma$ and k are to be evaluated for the most unstable mode. The anomalous resistivity is computed from the simulation results by dividing the Y -averaged electric field $\langle E_y \rangle_y$ by the current $\langle j_y \rangle_y$. These measurements are best done in region II where $\langle E_y \rangle_y$ is sizable. For example, at $T=80$, one finds $\langle E_y \rangle_y = 0.0022$ and $\langle j_y \rangle_y = 0.11$, giving $\eta = 0.25\omega_{p0}^{-1}$. By comparison the quasilinear result (1), using the simulation values for \mathcal{E}_F , ω , and k , gives $\eta = 0.24\omega_{p0}^{-1}$. In similar fashion the heating rates can be compared. In this case it is most convenient to compare values for $T < 70$, when $\dot{T}_{ex} = \dot{T}_{ey}$. For example, at $T=50$, one measures $\dot{T}_{ex}/T_{ex} \approx \dot{T}_{ey}/T_{ey} = 0.006$, while the quasilinear estimate, using a formula similar to (1), gives $\dot{T}_e/T_e = 0.0052$. The ion heating rate can also be compared. In this case theory predicts that little ion heating will occur; one finds that the ion temperature has increased by only 4% at $T=120$. Thus values for the anomalous resistivity and the heating rates found in the simulation are in good agreement with those calculated from quasilinear theory.

Finally, the question of the saturation mechanism is addressed. A useful rule of thumb for estimating when trapping can occur is to compare the trapping frequency $\omega_T = (eE_y k_y/m)^{1/2}$ (where $m = m_e$ for electron trapping, $m = m_i$ for ion trapping) and the maximum linear growth rate: $\gamma_{\max}/\omega_T \sim 1$ when trapping occurs.^{10,11} Using the saturation field to estimate the trapping frequency and taking γ_{\max} for the $n=4$ mode from the theo-

retical curve in Fig. 4, one finds $\gamma_{\max}/\omega_T = 0.84$ for the ions. Hence the fluctuation level is consistent with ion trapping as the saturation mechanism. However, by the time that saturation has occurred, the flutes have grown to such a size that boundary effects could be important. In this regard studies are presently underway which allow a larger X dimension and follow the instability farther into the saturation regime.

The authors would like to thank Clair Nielson for his invaluable advice and encouragement throughout the course of this work. We also thank R. C. Davidson, R. A. Gerwin, and N. T. Gladd for many helpful discussions. This research was supported by the U. S. Energy Research and Development Administration.

¹O. Buneman, Phys. Rev. 115, 503 (1959).

²C. T. Dum, R. Chodura, and D. Biskamp, Phys. Rev. Lett. 32, 1231 (1974).

³D. W. Forslund, R. L. Morse, and C. W. Nielson, Phys. Rev. Lett. 25, 1266 (1970).

⁴J. B. McBride, E. Ott, J. P. Boris, and J. H. Orens, Phys. Fluids 15, 2367 (1972).

⁵N. A. Krall and P. C. Liewer, Phys. Rev. A 4, 2094 (1971).

⁶C. W. Nielson and H. R. Lewis, to be published.

⁷D. W. Hewett, C. W. Nielson, and D. Winske, to be published.

⁸N. T. Gladd, to be published.

⁹R. C. Davidson and N. T. Gladd, to be published.

¹⁰W. M. Manheimer, Phys. Fluids 14, 579 (1971).

¹¹K. Papadopoulos, R. C. Davidson, J. M. Dawson, I. Haber, D. A. Hammer, N. A. Krall, and R. Shanny, Phys. Fluids 14, 849 (1971).

Electron Beam Generation in Plasma-Filled Diodes*

P. A. Miller, J. W. Poukey, and T. P. Wright

Sandia Laboratories, Albuquerque, New Mexico 87115

(Received 24 July 1975)

A study has been made of the response of low-density ($\sim 10^{13}$ cm⁻³) plasmas when subjected to the very high electric fields of relativistic-electron-beam-accelerator diodes. An anomalous resistive behavior has not been seen. Instead, sheath formation at the cathode and electron-beam generation across the sheath has been found. This has important applications to the design of diodes for future electron-beam machines.

Plasmas which occur in relativistic-electron-beam diodes are subject to average fields near 1 MV/cm. The behavior of these diode plasmas is of great importance because they can control electron-beam properties such as current densi-

ty, pinch formation, and pulse length. Previous studies have been made of the normally occurring high-density anode and cathode plasmas.¹ Here we report results of an experiment in which externally generated low-density ($n \sim 10^{13}$ /cm³) plas-

mas were injected into the diodes of electron-beam generators. It was found that the plasmas did not display an anomalous resistivity; instead, a collisionless sheath was found to form over the cathode, across which space-charge-limited flow of electrons and ions occurred. The sheath therefore constituted a virtual anode-cathode gap and the plasma behind the sheath behaved as a thick-anode plasma. The sheath-generation mechanism which is unambiguously identified here is closely related to that which probably occurs at lower fields and on longer time scales in some turbulent-heating experiments.²

At high currents, because no longitudinal magnetic field is applied, self-magnetic fields cause beam-electron flow to become two dimensional in nature. This regime will be discussed later. At lower currents, the flow is one dimensional and a very simple model adequately describes the plasma behavior. The model is of a planar-emitting electrode at very high voltage in a low-density, preformed, cold, collisionless plasma dominated by hydrogen. The electrode emits because a very thin surface layer of high-density cathode plasma is formed via the usual field-emission and whisker-explosion mechanisms,³ which may be aided here by ion bombardment. Diagnostic response times in the experiment were long enough so that oscillations at electron and ion plasma frequencies were not detected. The pulse duration was short enough, however so that a steady-state sheath was not reached. A sheath of thickness $x(t)$ was assumed to exist between the cathode plasma at voltage $-V(t) < 0$ and the field-free bulk plasma. Across this sheath flow space-charge-limited proton and electron currents given by

$$J_p = 1.86(4\epsilon_0/9)(2e/M)^{1/2}V^{3/2}x^{-2}, \quad (1)$$

$$J_e = (M/m)^{1/2}J_p, \quad (2)$$

where M and m are the proton and electron masses, $-e$ is the electron charge, and ϵ_0 is the vacuum permittivity. This nonrelativistic approximation is accurate for the one-dimensional work treated here.

The proton source is the cold plasma. If the proton current demanded by Eq. (1) is much greater than the saturation current

$$J_{ps} \sim ne(kT_e/M)^{1/2},$$

then the sheath boundary must move into the plasma to provide the proton flux.^{4,5} That is,

$$J_p = ne \, dx/dt. \quad (3)$$

At $t=0$, $x=0$ and the voltage pulse begins. If the driving voltage were a step function, the initial current would be infinite. Consequently it is necessary to take account of the characteristics of the voltage source in order to compute realistic V and I wave forms. The voltage source is a Nereus electron-beam machine⁶ which has a 1.9- Ω , 60-nsec pulse forming line which, here, is charged to 100 kV. The diode inductance is 45 nH and the main switch inductance is 15 nH. Equations (1) and (2) may be combined with the circuit equation for this machine equivalent circuit to obtain a first-order differential equation for I . This may then be iterated along with Eq. (3) to obtain solutions. Computed monitor voltage (assuming a scope rise time of 3 nsec) and diode current are shown in Fig. 1 for two typical plasma densities. Note that, in effect, the large electron current is being controlled by the much weaker ion current.

In the experiment, a 5-cm-diam brass cathode was driven by the electron-beam machine. The anode was made of copper screen wire, behind which was placed the apertured plasma source. Anode-cathode gaps from 1 to 6 cm were used. The plasma source was a $\frac{1}{2}$ -mm vacuum arc discharge across a ceramic surface which was coated with hydrocarbons (oil). The plasma density $n(r,t)$ and velocity were reproducible generally to better than 10%. Plasma temporal and spatial density measurements were made with apertured Faraday cups, floating double probes, and a 35-GHz interferometer. The plasma pulse typically was 5 μ sec wide and moved at 1.3 cm/ μ sec with some dispersion. The electron temperature (not measured directly) was probably only a few eV

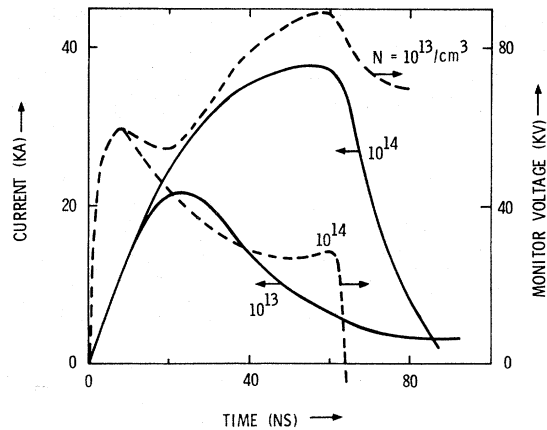


FIG. 1. Calculated machine voltage and current wave forms for two typical plasma densities.

as is typical for this type of source. The density in the gap was varied by changing the distance from the source to the anode (typically 8 cm), the charge voltage on the driving capacitor (0.25 μ F at typically 10 kV), and the relative timing of the discharge and the electron-beam pulse. Experimental wave forms are shown in Fig. 2. They agree quite well with the calculations in both shape and absolute amplitude. The machine polarity was reversed to check on electrode effects and to see if the direction of plasma flow was important; no change was observed.

In order to confirm that a beam of electrons was being formed with the full gap voltage, ratio-detector measurements of bremsstrahlung emission were made.⁷ Two x-ray *p-i-n* diodes viewed the anode through the 13-mm Lucite vacuum wall. A 0.25-mm copper filter was placed in front of one diode, so that the two diodes responded to x rays above roughly 30 and 45 keV, respectively. The ratio of the diode signals (at the peak power point in the pulse) is plotted as a function of corrected gap voltage in Fig. 3. Shots with a wide range of currents and plasma densities are represented. Also shown for reference are ratios from shots with small anode-cathode gaps and no injected plasma present, conditions under which normal beam generation occurs. Measurements taken with a harder filter gave similar results. We conclude that indeed an electron beam with essentially the full gap voltage ($\pm \sim 10\%$) arrives at the anode. It is evident that this x-ray spectral measurement, along with the excellent agreement between calculated and measured current ampli-

tudes and pulse shapes, effectively verify the sheath model. Attempts to obtain satisfactory alternate explanations involving turbulence, run-away production, etc., have not been successful.

Two-dimensional effects become important in flow in high-aspect-ratio diodes when the current approaches the critical pinch current, i.e., when the Larmor radius of beam electrons approaches the anode-cathode gap thickness. Experimental runs were performed with Nereus under conditions where pinched flow occurred, as indicated by anode damage and pinhole x-ray photographs. A pinch was obtained at 100 kV, 50 kA, with an 11-mm gap. A numerical simulation of pinched electron flow was performed using a time-independent code described previously⁸ for this case; a 1-mm-thick cathode-sheath region was required to match the experimentally measured current in the middle of the pulse. The plasma was assumed to exclude electric but not magnetic fields. It was found in the simulation that 50% of the current pinched to a 5-mm-diam spot at the anode. In the experiment, both the hole diameter in the anode and the spot size in the time-integrated x-ray photograph were 5 mm, in agreement with the simulation result. This suggests that magnetic fields do penetrate the plasma, as the model assumes. Measurements performed with a glass-enclosed magnetic probe in a much thicker anode plasma also showed magnetic fields present in the plasma. It was observed that the current pulse had a substantially different shape than in the one-dimensional-flow case, such that the diode impedance was nearly constant in time.

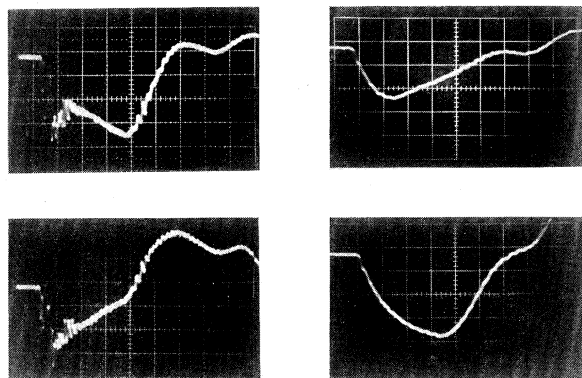


FIG. 2. Sample monitor voltage and diode-current signals. Top: $n \sim 3 \times 10^{13}/\text{cm}^3$, voltage at left (20 kV/division) and current at right (13 kA/division); bottom: $n \sim 10^{14}/\text{cm}^3$. All sweeps 20 nsec/division. Anode-cathode gap = 2 cm.

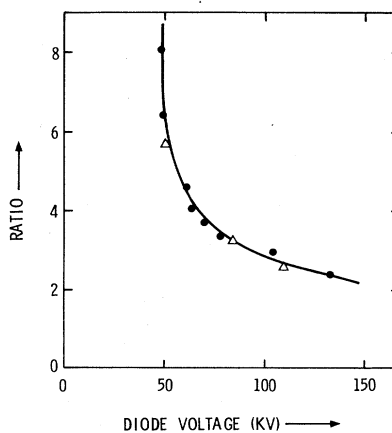


FIG. 3. Ratio-detector results. Dots represent plasma shots; triangles represent short-gap no-plasma reference shots.

This means that a fixed line impedance could be matched closely by the plasma-filled diode, thus giving efficient energy extraction. At present, no simple model for the time-dependent sheath and beam behavior in the two-dimensional case has been obtained.

The same type of plasma-filled-diode experiment subsequently was run with the Hydra accelerator. Using a 12.7-cm-diam cathode and a 2.6-cm anode-cathode gap, pinches could be obtained in substantial agreement with simulation predictions (at nominally 625 kV and 275 kA). A typical sheath thickness required in the simulation to match the experimentally measured current in the middle of the pulse was 0.6 cm. Furthermore, the diode impedance was relatively constant in time and could be lowered at will by injection of higher-density plasma which led to formation of a thinner sheath.

In some experiments with Nereus, the anode-cathode gap was opened up to as much as 6 cm. It was found that beams were generated when adequate plasma filling was employed. It is not known how the high- (v/γ) beams thus generated were able to traverse the thick-plasma region. Radial electric fields at the plasma column edge and hollow beam profiles may have been involved.

In summary, the behavior of low-density plasmas subject to very high electric fields has been investigated. Electron-beam generation due to sheath formation has been observed. In the one-dimensional case, the sheath behavior is easy to model. In work with axial diode plasmas, the behavior of the plasma may be somewhat different than previously was supposed.⁹⁻¹² Implications of these results for electron-beam work are the following: (1) A convenient way has been found to generate a well-behaved anode plasma. This is valuable for use with future generations of short-pulse electron-beam machines applied to pellet-fusion work. With such machines, use of beam energy to create anode plasma is undesirable because of energy and time considerations. (2) Use of plasma-filled diodes allows one to adjust diode impedance independently of electrode

configuration. Low diode impedances can be obtained without encountering the closure problems which normally accompany the use of short anode-cathode gaps. Ultimate limits to this technique are not known.

*Work supported by the U. S. Energy Research and Development Administration.

¹M. Farber, J. E. Robin, and R. D. Srivastava, *J. Appl. Phys.* **43**, 3313 (1972); L. P. Mix, J. G. Kelly, G. W. Kuswa, D. W. Swain, and J. N. Olsen, *J. Vac. Sci. Technol.* **10**, 951 (1973); J. G. Kelly and L. P. Mix, *Appl. Phys. Lett.* **46**, 1084 (1975); I. Langmuir, *Phys. Rev.* **33**, 954 (1929).

²E. I. Lutsenko, N. D. Sereda, and L. M. Kontsevoi, *Zh. Eksp. Teor. Fiz.* **67**, 979 (1974), and references therein.

³G. A. Mesyats, E. A. Litvinov, and D. I. Proskurovsky, in *Proceedings of the Fourth International Symposium on Electrical Insulation in Vacuum, Waterloo, Ontario, Canada, 1970* (Univ. of Waterloo, Ontario, Canada, 1970), p. 82; R. K. Parker, R. E. Anderson, and C. V. Duncan, *J. Appl. Phys.* **45**, 2463 (1974).

⁴F. F. Chen, in *Plasma Diagnostic Techniques*, edited by R. H. Huddelstone and S. L. Leonard (Academic, New York, 1965), Chap. 4.

⁵M. M. Widner, I. Alexeff, W. D. Jones, and K. E. Lonngren, *Phys. Fluids* **13**, 2532 (1970).

⁶K. R. Prestwich, *IEEE Trans. Nucl. Sci.* **18**, No. 3, 493 (1971).

⁷J. V. Walker and J. Stevens, *Rev. Sci. Instrum.* **45**, 163 (1974).

⁸J. W. Poukey, J. R. Freeman, and G. Yonas, *J. Vac. Sci. Technol.* **10**, 954 (1973); J. W. Poukey and A. J. Toepfer, *Phys. Fluids* **17**, 1582 (1974).

⁹S. L. Nedoseev, V. P. Smirnov, A. M. Spektor, and D. G. Fil'kin, *Zh. Tekh. Fiz.* **42**, 2520 (1972) [*Sov. Phys. Tech. Phys.* **17**, 1961 (1973)].

¹⁰G. Yonas, K. R. Prestwich, J. W. Poukey, and J. R. Freeman, *Phys. Rev. Lett.* **30**, 164 (1973).

¹¹P. A. Miller, J. Chang, and G. W. Kuswa, *Appl. Phys. Lett.* **23**, 423 (1973).

¹²G. Yonas, J. W. Poukey, K. R. Prestwich, J. R. Freeman, A. J. Toepfer, and M. J. Clauser, *Nucl. Fusion* **14**, 731 (1974).

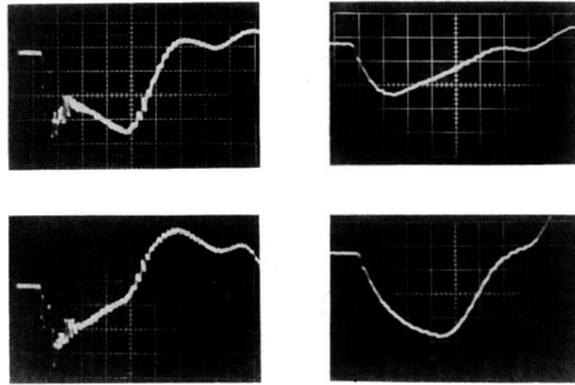


FIG. 2. Sample monitor voltage and diode-current signals. Top: $n \sim 3 \times 10^{13}/\text{cm}^3$, voltage at left (20 kV/division) and current at right (13 kA/division); bottom: $n \sim 10^{14}/\text{cm}^3$. All sweeps 20 nsec/division. Anode-cathode gap = 2 cm.